

# Effect of 5-methylcytosine on the stability of triple-stranded DNA—a thermodynamic study

Luigi E.Xodo, Giorgio Manzini, Franco Quadrifoglio<sup>1</sup>, Gijs A.van der Marel<sup>2</sup> and Jacques H.van Boom<sup>2</sup>

Department of Biochemistry, Biophysics and Macromolecular Chemistry, University of Trieste, I-34127 Trieste, <sup>1</sup>Institute of Biology, Faculty of Medicine, University of Udine, I-33100 Udine, Italy and <sup>2</sup>Gorlaeus Laboratories, University of Leiden, The Netherlands

Received July 12, 1991; Revised and Accepted September 26, 1991

## ABSTRACT

We have previously shown that the pyrimidine oligonucleotide 5'CTTCCTCCTCT (*Y11*) recognizes the double-helical stem of hairpin 5'GAAGGAGGAG-A-T<sub>4</sub>-TCTCCTCCTTC (*h26*) by triple-helix formation (1). In this paper, we report the effect on triplex formation of substituting the cytosine residues of *Y11* with 5-methylcytosines (*5meY11*). In addition, we have studied the thermodynamics of the interaction between *h26* and *5meY11*. The results can be summarised as follows: (i) gel electrophoresis shows that at T = 5°C and pH 5, both *Y11* and *5meY11* form DNA triple helices with *h26*, whereas at pH 6.8 only the methylated strand binds to *h26*; (ii) pH-stability curves of the DNA triplexes formed from *h26* + *Y11* and *h26* + *5meY11* show that *Y11* and *5meY11* are semi-protonated at pH 5.7 and 6.7, respectively. Thus, it is concluded that cytosine methylation expands the pH range compatible with triplex formation by one pH unit; (iii) as the unmethylated triplex (*h26:Y11*), the methylated one (*h26:5meY11*) denatures in a biphasic manner, in which the low temperature transition results from the dissociation of *5meY11* from *h26*. The T<sub>m</sub> of the triplex to *h26* plus *5meY11* transition is strongly enhanced (about 10°C) by cytosine methylation. A van 't Hoff analysis of denaturation curves is presented; (iv) DSC experiments show that triplex formation between *5meY11* and *h26* is characterized by  $\Delta H = -237 \pm 25$  kJ/mol and  $\Delta S = -758 \pm 75$  J/Kmol, corresponding to an average  $\Delta H$  of  $-21$  kJ/mol and  $\Delta S$  of  $-69$  J/Kmol per Hoogsteen base pair; (v) the thermodynamic analysis indicates that the extra stability imparted to the triplex by methylcytosine is entropic in origin.

## INTRODUCTION

Recent research has shown that homopyrimidine oligodeoxynucleotides can recognize the major groove of homopurine-homopyrimidine DNA double helices, forming

triple-stranded structures (2–6). The homopyrimidine oligonucleotide (Hoogsteen strand) is parallel bound to the purine strand of the target duplex, by means of Hoogsteen pairs (7). The resulting DNA triplex is stabilized by T:A:T and C:G:C<sup>+</sup> triads (8–11). Since the latter pairing requires the protonation of the cytosine residues of the Hoogsteen strand, the triplex becomes stable only at acidic conditions.

Homopurine-homopyrimidine stretches are widespread in eukaryotic genomes and they are often located in positions flanking the genes (12). In the presence of superhelical stress and pH below 7 these sequences can adopt an intramolecular triplex structure (H-DNA), in which half of the pyrimidine strand binds the tract left in double-stranded form (12–16). Hence, the formation of triple-stranded DNA is believed to play a role in the regulation of transcription (12,17).

Interest in DNA triplex is growing since homopyrimidine oligodeoxynucleotides (i) may be used as 'antisense' DNA in chemotherapy, in which gene expression can be influenced by triple helix formation (18); (ii) may be covalently linked to a DNA cleaving agent such as EDTA-Fe(II) to generate artificial nucleases useful in chromosome mapping (3,19).

An essential point for the use of homopyrimidine oligodeoxynucleotides as 'antisense' compounds is that they should form stable triplexes at physiological conditions. However, stabilization of C+G containing triple-stranded structures is induced only by acidic pH. Therefore, to achieve stabilization at neutral pH, the Hoogsteen homopyrimidine strand should be modified. Methylation of cytosine residues has proved to induce stabilization of poly(dTd5meC).poly(dGdA).poly(dTd5meC) at physiologic pH (20), thus alkylation of the Hoogsteen strand could be important to extend the pH range compatible with triple formation. In order to investigate the effect of methylcytosine on triple-stranded DNA, we have studied in detail the interaction between a Watson-Crick DNA helix with a homopyrimidine strand in which the cytosines have been substituted with 5-methylcytosines. The comparison of the results reported in this paper with those previously obtained for triplex structures made by unmethylated oligomers (1,21) allows a precise quantification of the effect of 5-methylcytosine on triple-stranded DNA.

## MATERIALS AND METHODS

### Samples

The chemical synthesis of the oligodeoxynucleotides used in this study:

*h26* d(GAAGGAGGAGATTTTTCTCCTCCTTC)  
*5meY11* d(5meCTT5meC5meCT5meC5meCT5meCT)  
*Y11* d(CTTCCTCCTCT)

was performed in solid phase, using a modified phosphotriester method (22). After base deprotection, the oligonucleotides were purified by gel-filtration chromatography (Sephadex G-25) using as eluent a 5 mM solution of ammonium hydrogen carbonate. Purity was checked by anion exchange HPLC (gradient used was 0–1 M NaCl in 12 mM NaOH, pH=12, in 60 min, at 1ml/min).

### Buffers

Electrophoreses were carried out in 50 mM Tris-acetate, 50 mM NaCl, 5 mM MgCl<sub>2</sub>, pH 5, 6, 6.8 and 7. pH-Stability curves were determined in 50 mM MES, 10 mM MgCl<sub>2</sub>, 100 mM NaCl.

For uniformity with our previous studies on DNA triplex structures (in sodium-acetate at pH 5) (1), ultraviolet absorption and DSC experiments were carried out in sodium-acetate 100 mM, NaCl 50 mM, MgCl<sub>2</sub> 10 mM, pH fixed from 5 to 6, as specified in the figure captions. The buffer capacity of sodium-acetate 100 mM at pH 6 is sufficiently strong to perform thermal experiments: in the temperature range 15–90°C, the apparent pH of DNA solutions in 100 mM sodium-acetate at pH 5 and 6 were found to vary only by 0.05 units.

### Gel Electrophoresis

Non-denaturing gels (29:1, acrylamide:bisacrylamide) were made polymerizing overnight a 20% acrylamide solution in 20×10×0.7 mm slabs. The samples were equilibrated overnight in the appropriate buffer and, before loading, an equal amount of buffer containing 50% sucrose was added. Gels were run at a constant current of 20 mA. Electrophoreses were stopped when bromphenol blue had migrated for 15 cm. DNA bands were stained with 'stains-all' in formamide:water 1:1, and photographed with a polaroid camera.

### UV Thermal Denaturations

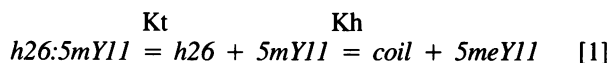
Ultraviolet absorbance spectra were recorded with a Cary 219 (Varian) spectrophotometer equipped with a thermostatted cuvette holder. The DNA concentration was determined by UV absorbance measurements (260 nm) at 95°C, using for the DNA coil state the following extinction coefficients: 7500, 8500, 12500 and 15000 M<sup>-1</sup>cm<sup>-1</sup> for C (5meC), T, G and A, respectively (23). The denaturations were performed raising the temperature at the rate of 0.5°C/min, by means of a Haake PG 20 temperature programmer, connected with a Haake water circulating bath.

### Mixing curves

Mixing curves of *h26* with *5meY11* were obtained in 100 mM sodium-acetate (pH 6), with the method of continuous variation (24). Equimolar solutions of *h26* and *5meY11* were prepared and mixed together at increasing *5meY11/h26* ratios, keeping constant the total DNA concentration. This was accomplished by adding amounts of *Y11* to *h26*, and vice-versa. At each DNA ratio the UV spectrum of the mixture was recorded. UV absorbance at 264 nm was then plotted versus the molar fraction of *Y11*.

### Analysis of transition data from UV absorption

Considering that the process of triple helix formation from *h26* and *5meY11* is bimolecular, the energetics of this reaction was evaluated from UV melting curves as follows. The dissociation of the triple-stranded structure can be written as:



where  $K_t$  and  $K_h$  are the equilibrium constants for the triplex to hairpin plus single strand transition (transition 1) and hairpin to coil (transition 2), respectively. Assuming that transition 1 occurs in a two-state fashion,  $K_t$  is given by:

$$K_t = \alpha^2 C_t / (1-\alpha) = \exp(-\Delta H_t / RT + \Delta S_t / R) \quad [2]$$

where  $\alpha$  is the fraction of dissociated *5meY11*,  $C_t$  is the strand concentration of *5meY11* (equal to that of *h26*) and  $H_t$  and  $S_t$  are the enthalpy and entropy changes of triplex disruption. Since transition 1 is bimolecular, the value of  $\alpha$  at which the differential melting curves,  $dA/dT$  versus  $T$ , reach their maxima ( $T=T_{max}$ ) is 0.58. At  $T=T_{max}$ , equation 2 becomes:

$$1/T_{max} = -R \ln C_t / \Delta H_t + (0.222 R + \Delta S_t) / \Delta H_t \quad [3]$$

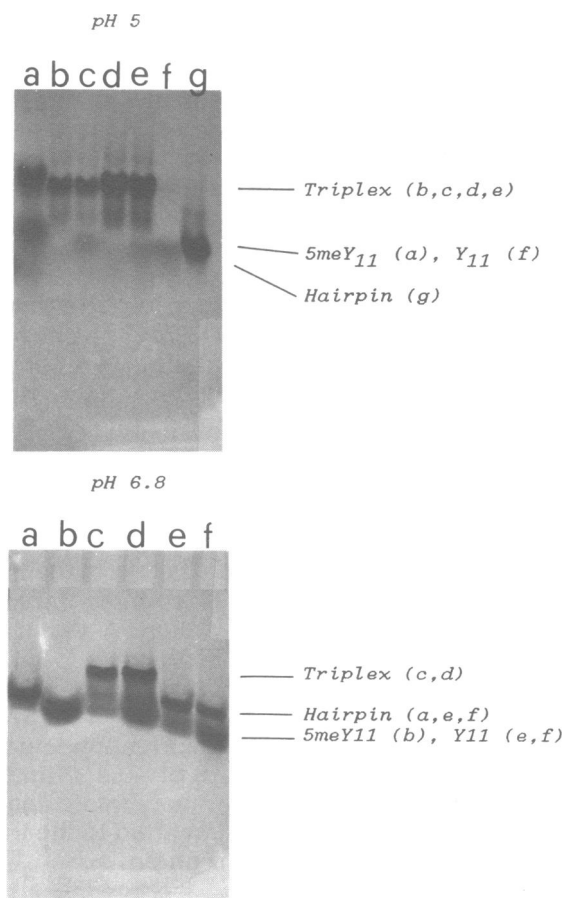


**Figure 1.** Polyacrylamide gel electrophoresis of equimolar mixtures *h26:5meY11* and *h26:Y11* at pH 5 and 6.8,  $T=5^\circ\text{C}$ . At pH 5, *5meY11* (lane a): it migrates with two bands of which the one at low mobility is a dimeric form of *5meY11* stabilized by C:C+ base pair; *h26:5meY11* (lanes b,c); *h26:Y11* (lanes d,e); *Y11* (lane f) and *h26* (lane g). At pH 6.8, *h26* (lane a); *5meY11* (lane b); *h26:5meY11* which forms a triplex (lanes c,d); *h26:Y11* which does not form a triplex (lanes e,f).

The plot of  $1/T_{max}$  vs  $\ln C_t$  is linear and allows to estimate from the slope and y-intercept the  $\Delta H_t$  and  $\Delta S_t$  parameters for the transition. Errors on  $\Delta H_t$  and  $\Delta S_t$  are 10%. The free energy of triplex formation was obtained from the standard equation:

$$\Delta G_t = \Delta H_t - T\Delta S_t \quad [4]$$

### Differential Scanning Calorimetry (DSC)

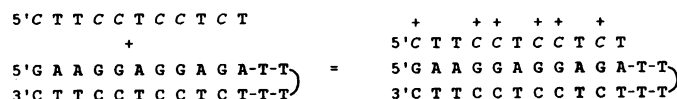
Differential scanning calorimetry was carried out with a Setaram microcalorimeter. A scan rate of  $0.5^\circ\text{C}/\text{min}$ , from 20 to  $95^\circ\text{C}$ , was used in both denaturation and renaturation cycles. The sample cuvette contained  $\approx 0.9$  ml of DNA at a concentration in the range 100–200  $\mu\text{M}$  of triplex (or hairpin *h26*). Instrument baseline, obtained in both denaturation and renaturation steps with the cells filled with sodium-acetate 100 mM (pH 6), was deducted from each DNA thermogram. Error on  $\Delta H_t$  and  $\Delta S_t$  from DSC curves is at most 10%.

## RESULTS

### Gel electrophoresis: triple helices are formed at different pH

The electrophoretic mobilities of equimolar mixtures *h26:5meY11* and *h26:Y11* were analyzed in 20% polyacrylamide gels, in 50 mM Tris-acetate, 20 mM NaCl, 10 mM  $\text{MgCl}_2$ , at pH 5, 6, 6.8 and 7. Figure 1 shows typical electrophoretic profiles of *h26*, *5meY11*, *Y11* and *h26:5meY11*, *h26:Y11* at pH 5 and 6.8,  $T=5^\circ\text{C}$ . The samples, before PAGE analysis, were dissolved in the appropriate buffer, heated at  $80^\circ\text{C}$  for 15 min. and let

overnight to cool at room temperature. Sequence *h26* migrates as a 12-mer duplex since it assumes a hairpin form. At pH 5 both mixtures *h26:5meY11* and *h26:Y11* migrate with a slow moving band, as compared to the mobility of *h26*, which is attributed to the formation of a triple helix (Scheme I)(1). This is to be expected since a triple helix has a larger diameter than a double helix, as well as a lower negative charge density (effect of protonated  $5\text{meC}^+$ ). At pH 6.8 the two mixtures exhibit different electrophoretic profiles. While *h26:5meY11* practically migrates as a triplex (only a small amount of *h26* having loses the Hoogsteen strand), *h26:Y11* does not form any triplex at this pH. This shows that, when the Hoogsteen strand is methylated, the pH range suitable for triplex formation is extended to near neutrality.



Scheme I. (C = 5-methyl-cytosine)

### pH-Effect on triplex formation: stability curves

In order to precisely quantify the effect of methylcytosine on triple helix formation we have determined pH stability curves for *h26:5meY11* and *h26:Y11* at room temperature. By measuring the UV absorbance (260 nm) of mixtures *h26:5meY11* and *h26:Y11* in 50 mM NaCl, 10 mM  $\text{MgCl}_2$ , as a function of pH, the curves of Figure 2 are obtained. For pH values higher than 7.5 the UV absorbance of the mixtures does not change significantly. Below 7.5, a hypochromic effect is observed since the pyrimidine strands (*5meY11* and *Y11*) bind to the major groove of *h26* forming DNA triple helices. These pH-induced transitions result from protonation at N3 of cytosine in *5meY11* and *Y11* to form Hoogsteen pairs with the Watson-Crick C:G pairs of *h26* (Scheme I). From these plots it can be seen that hairpin to triplex formation is accompanied by a net hypochromic effect of about 10%. From the pH-stability curves one finds that in the presence of *h26* the methylated strand *5meY11* is semiprotonated at pH 6.8, and the unmethylated *Y11* at pH 5.8. This shows that methylation extends the pH range for triplex formation of one unit. The pH induced hairpin to triplex transition

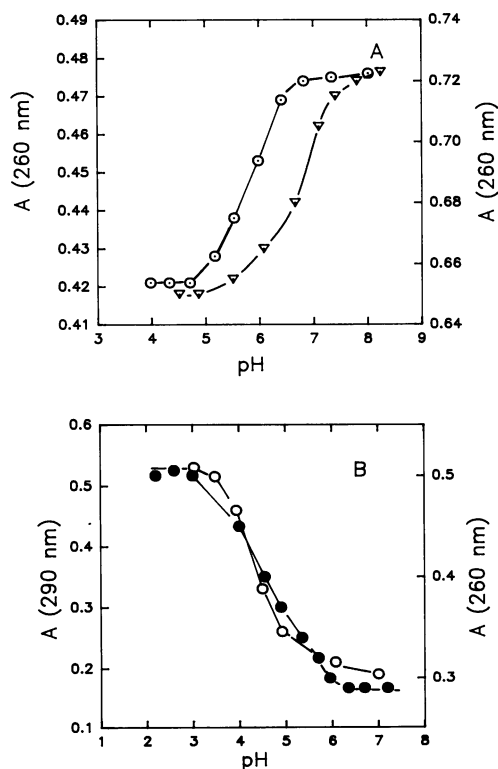


**Figure 2.** (A) pH-Stability curves for *h26:5meY11* ( $\nabla$ ) and *h26:Y11* ( $\odot$ ) in 50 mM NaCl, 10 mM  $\text{MgCl}_2$ , room temperature. In ordinate it is reported the hypochromic effect observed as the pH of equimolar solutions of *h26+Y11* and *h26+5meY11* is lowered; (B) Protonation curves for *Y11* ( $\circ$ ) and *5meY11* ( $\bullet$ ), obtained from UV-absorbance experiments as a function of pH, at  $T=45^\circ\text{C}$  (to prevent strand self-association): the  $\text{pK}_a$  of both *Y11* and *5meY11* is  $4.4 \pm 0.2$ .

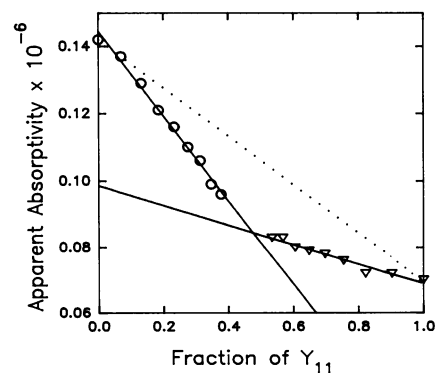


**Figure 3.** Mixing curve for the interaction between *h26* with *5meY11* in 100 mM sodium-acetate (pH 6), 50 mM NaCl, 10 mM  $\text{MgCl}_2$ . Molar (strand) absorptivity data have been plotted at 240 nm, where a good hypochromic effect is observed. Dotted line is expected in absence of interaction between *h26* and *5meY11*.

is cooperative: a variation of 0.5 units from the semi-protonation point of the Hoogsteen strand creates conditions in which the triple helix is strongly stabilized or destabilized. We have also measured the pKa's of single-stranded *5meY11* and *Y11* individually, finding that they are similar and equal to  $4.4 \pm 0.2$ , as shown by Figure 2B (1).

In accord with electrophoresis, at pH 5 both mixtures *h26:5meY11* and *h26:Y11* adopt a triple-stranded form, whereas at pH=6.8 only *h26:5meY11* does form a DNA triplex.

#### Stoichiometry of *h26:5meY11* from UV mixing curves

Before studying the energetics of association between *h26* and *5meY11* in 100 mM sodium-acetate (pH 6), 50 mM NaCl, 10 mM MgCl<sub>2</sub>, we determined the stoichiometry of the complex *h26:5meY11*, by the method of continuous variation (24). Figure 3 shows the UV absorbance changes which result from continuous addition of *5meY11* to *h26* and vice-versa, while keeping constant the total DNA concentration. The data of each titration were fitted with two straight lines which intersected at the point in which the mole fraction of *5meY11* is 0.48. This result indicates that mixture *h26:5meY11* does form in the chosen buffer a complex with a 1:1 stoichiometry.

#### Denaturation of the DNA triplex

As observed for *h26:Y11* (1), the methylated triplex *h26:5meY11* melts in two distinct steps, as clearly demonstrated by  $dA/dT$  versus  $T$  plots (Figure 4). The low-temperature transition (transition 1) is found to depend on the DNA concentration, while the high-temperature one (transition 2) is concentration independent. Thus, transition 1 reflects the dissociation of *5meY11* from *h26*, a bimolecular process, while transition 2 is due to the

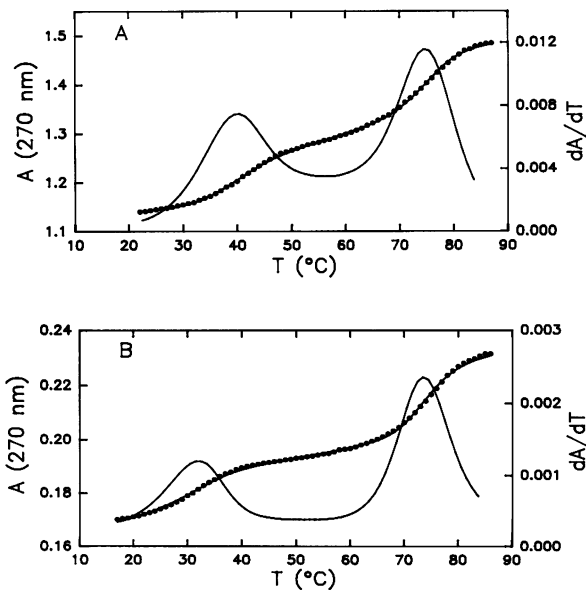


**Figure 4.** Thermal denaturations of the triplex *h26:5meY11* in 100 mM sodium-acetate (pH 6), 50 mM NaCl, 10 mM MgCl<sub>2</sub>. The hollow circles are the experimental absorbances (270 nm) as a function of  $T$ . Differential ( $dA/dT$  vs  $T$ ) and nonlinear best-fit (NLS) (—) curves are also reported. The DNA concentrations are 24.4 (A) and 1.5 (B)  $\mu\text{M}$  in triplex. The NLS curves were obtained applying a tree-state model to the equilibria in eq. [1], fixing  $S_i$  and  $\Delta H_i$  to the values obtained from  $1/T_{\text{max}}$  vs  $\ln C_p$ , and leaving  $\Delta H_h$ ,  $\Delta S_h$ , pre- and post-transition slopes as adjustable parameters. A detailed description of the method is reported by Ref.1.

denaturation of hairpin *h26*, a unimolecular process (1). The thermally induced hyperchromicities observed in the UV denaturations are  $10(\pm 1)\%$  for transition 1 and  $15(\pm 2)\%$  for transition 2.

Since protonation is involved in triplex formation, transition 1 should depend on the pH much more than transition 2. We have melted *h26:5meY11* at different pH values between 5 and 6 and observed that, while the midpoint ( $T_m$ ) of transition 2 is slightly affected by the pH variation (only near pH 5 the  $T_m$  of transition 2 decreases from 74 to 72°C), the  $T_m$  of transition 1 is strongly dependent on pH: 36°C (pH 6); 43°C (pH 5.8); 51°C (pH 5.4); 56°C (pH 5.2) and 62°C (pH 5). This behaviour is in keeping with the formation of protonated C:G:C<sup>+</sup> triads on binding *5meY11* to *h26*.

The clear dependence of transition 1 from the DNA concentration was utilized to evaluate the thermodynamic

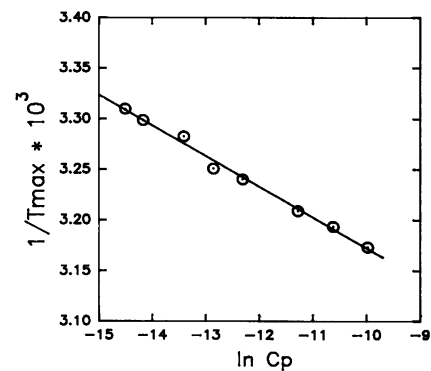


**Figure 5.** Plot of  $1/T_{\text{max}}$  vs  $\ln C_p$  for *h26:5meY11* triplex in 100 mM sodium-acetate (pH 6), 50 mM NaCl, 10 mM MgCl<sub>2</sub>. DNA concentration varies from 0.5 to 46  $\mu\text{M}$  in triplex. Linear regression of the data gives a slope of  $-0.0303$  and a y-intercept of 0.00287.

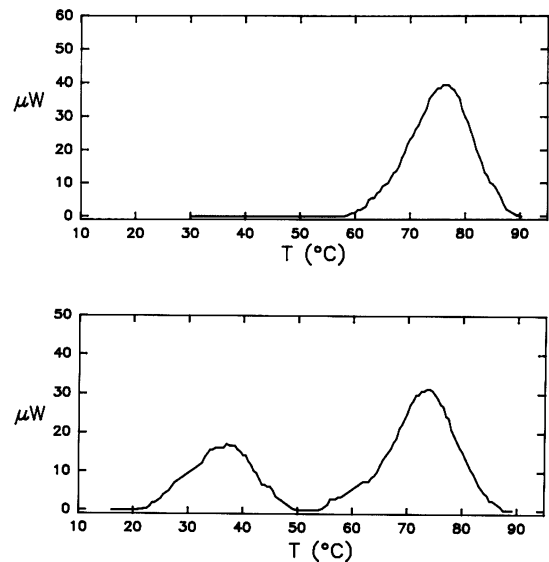


**Figure 6.** (Top) DSC curve of hairpin *h26* (0.173  $\mu\text{M}$  of *h26* in 0.865 ml of buffer); (Bottom) DSC curve obtained from mixture *h26+5meY11*, at strand ratio 1.15:1 (0.154  $\mu\text{M}$  di *h26* + 0.133  $\mu\text{M}$  di *5meY11* in 0.887 ml di buffer). Measurements were carried out in 100 mM sodium-acetate (pH 6), 50 mM NaCl, 10 mM MgCl<sub>2</sub>.

parameters for triplex disruption through a plot of  $1/T_{max}$  versus  $\ln C_t$ . In the concentration range of 0.5–46.0  $\mu\text{M}$ /triplex we obtained the plot of Figure 5. The  $T_{max}$  values were taken at the maximum of the corresponding  $dA/dT$  curves. Linear regression of the data gave a slope of  $-0.0303$  and a y-intercept of  $0.00287$ , from which the following parameters were obtained:

$$\Delta H_t = 274 \pm 30 \text{ kJ/mol}; \Delta S_t = 784 \pm 80 \text{ J/Kmol}$$

As transition 1 exhibits a good degree of cooperativity at all DNA concentration considered, an accurate determination of the  $T_{max}$  values was made possible. The experimental error involved in this method of analysis depends on the size of the explored DNA concentration range: with a 92-fold concentration range the estimated error is  $\pm 10\%$ .

### DSC analysis

We have also measured directly the enthalpy change of triple helix formation from *h26* and *5meY11* by differential scanning calorimetry (DSC). Figure 6 shows typical DSC curves for the denaturations of double-stranded *h26* and triple-stranded *h26:5meY11*, in 100 mM sodium-acetate (pH 6). Baselines have been deducted from the DSC curves. In accord with UV denaturations, the thermogram of *h26* is characterized by only one transition, whereas the thermogram of *h26:5meY11* exhibits two peaks which match those shown by optical meltings. Rescanning gave DSC curves which were superimposable, indicating that both transitions 1 and 2 are reversible, at a heating rate of  $0.5^\circ\text{C}/\text{min}$ . Integration of the area under the DSC curves gives the enthalpy changes of hairpin and triplex formation (from the corresponding  $\Delta C_p$  versus  $dT$  curves) whereas the entropy

**Table I.** Thermodynamic parameters for transitions *h26* = coil and *h26:5meY11* = *h26* + *5meY11*, in sodium-acetate 100 mM (pH 6), NaCl 50 mM, MgCl<sub>2</sub> 10 mM<sup>(a)</sup>.

Denaturations of host hairpin <i>h26</i> <sup>(b)</sup>					
Sample	Conc. $\mu\text{M}/\text{triplex}$	$\Delta H_h$ kJ/mol	$\Delta S_h$ J/Kmol	$\Delta G_h$ kJ/mol	Method
<i>h26</i>	5.7	322	915	49	UV
<i>h26</i>	196.5	378	1080	56	DSC
Denaturation of triplex <i>h26:5meY11</i>					
(A) From slope of $1/T_{max}$ versus $\ln C_t$ <sup>(c)</sup>					
Sample	Conc. $\mu\text{M}/\text{triplex}$	T $^\circ\text{C}$	$\Delta H_t$ kJ/mol	$\Delta S_t$ J/Kmol	$\Delta G_t$ kJ/mol
<i>h26:5meY11</i>	0.5	29.0	274	784	40
<i>h26:5meY11</i>	0.7	30.0			
<i>h26:5meY11</i>	1.5	31.5			
<i>h26:5meY11</i>	2.6	34.5			
<i>h26:5meY11</i>	4.4	35.0			
<i>h26:5meY11</i>	12.6	38.5			
<i>h26:5meY11</i>	24.4	40.2			
<i>h26:5meY11</i>	46.0	42.0			
(B) From DSC measurements <sup>(d)</sup>					
	Conc. $\mu\text{M}/\text{triplex}$	$\Delta H_t$ kJ/mol	$\Delta S_t$ J/Kmol	$\Delta G_t$ kJ/mol	
<i>h26:5meY11</i>	149	239	764	11	
<i>h26:5meY11</i>	149	229	730	11	
<i>h26:5meY11</i>	149	243	780	10	

(a)  $\Delta H_t$ ,  $\Delta S_t$  and  $\Delta G_t$  are given as round number;  $\Delta G_t$  is calculated at  $25^\circ\text{C}$ , with the assumption that  $\Delta H_t$  and  $\Delta S_t$  do not depend on temperature ( $\Delta C_p=0$ ); (b)  $\Delta H_h$  and  $\Delta S_h$  of hairpin denaturation have been obtained from nonlinear least-square analysis of UV-melting curves as previously described (32) and from DSC measurements; (c) analysis has been carried out using  $T_{max}$  values obtained only from renaturation curves: errors on  $\Delta H_t$  and  $\Delta S_t$  are  $\pm 10\%$ , on  $T_{max}$  is  $0.5^\circ\text{C}$ ; (d) errors on  $\Delta H_t$  and  $\Delta S_t$  from DSC are at most 10%.

changes were computed by the area under the corresponding  $\Delta C_p/T$  versus  $T$  curves. The average values from three scannings are:

$$\Delta H_t = -237 \pm 24 \text{ kJ/mol}; \Delta S_t = -758 \pm 75 \text{ J/Kmol}$$

The enthalpy value is 15% lower than the corresponding van 't Hoff  $\Delta H_t$ , obtained from  $1/T_{max}$  vs  $\ln C_t$ . This agreement can be regarded as satisfactory, considering that the method of analysis based on  $1/T_{max}$  vs  $\ln C_t$  assumes that: (i) transition 1 occurs in an all-or-none fashion; (ii) transition 1 is perfectly reversible; (iii)  $\Delta H_t$  and  $\Delta S_t$  are temperature independent, i.e. the specific heat capacities of the triplex and *h26* plus *5meY11* states are the same.

The DSC  $\Delta H_t$  is reasonably in accord with that previously obtained for an intramolecular triple structure mimicking the H-DNA conformation (21).

The results obtained from the thermodynamic analyses are collected in Table I.

### DISCUSSION

Although the apparent pKa's of *5meY11* and unmethylated *Y11* are  $4.4 \pm 0.2$ , only the mixture between *h26* and *5meY11* is able to form a DNA triplex near neutrality. This is clearly shown by gel electrophoresis at pH 6.8 (Figure 1). The pH-stability curves, obtained at room temperature, show that, in the presence of host helix *h26*, the semiprotonation of *5meY11* (pH=6.8) shifts one unit higher with respect to that of *Y11* (pH=5.8), since protonation is, in this case, accompanied by triple helix formation. Thus, these experiments clearly show that substitution of cytosine with 5-methylcytosine in *Y11* extends the pH range compatible with triple helix formation up to near neutrality. This piece of evidence suggests that 5-methylcytosine is an important structural element for inducing stabilization of (C+G) containing triple helices at physiological conditions. The effect of methylcytosine on triple-helix formation was first observed in polynucleotide structures: it was found that, while poly(dTdm5C).poly(dGdA).poly(dTm5dC) forms a triplex structure even at pH near 8, the unmethylated analog poly(dTdc).poly(dGdA).poly(dTdc) requires lower pH (20).

Another important factor emerging from this study is that cytosine methylation strongly enhances triplex stability. In 100 mM sodium-acetate (pH 5), at DNA triplex concentration of 6

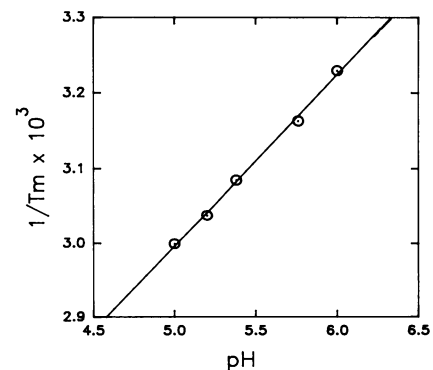


**Figure 7.** Dependence of the thermal midpoint ( $T_m$ ) of the triplex to *h26* plus *5meY11* transition from pH, in 50 mM NaCl, 10 mM MgCl<sub>2</sub>. Linear regression of the data gives a slope of  $2.28 \times 10^{-4}$ .

$\mu\text{M}$ , the thermal midpoint of transition  $h26:5meY11 = 5meY11 + h26$  is  $62^\circ\text{C}$ , while that of  $h26:Y11 = Y11 + h26$  is  $52^\circ\text{C}$ . This finding may be helpful for designing therapeutical *antisense* oligonucleotides aimed to influence the expression of a target gene via triple-helix formation (18). For this application it is important that the pyrimidine strand strongly hybridizes the target DNA at  $37^\circ\text{C}$ . A higher stability of DNA triplexes containing 5-methylcytosines has also been observed by Maher et al. through restriction endonuclease protection experiments (25).

The enhanced triplex stability imparted by the methylation of the third pyrimidine strand appears to be entropic in origin: in fact, the  $\Delta H_t$  relative to the formation of the methylated  $h26:5meY11$  triplex is not higher than the  $\Delta H$  obtained, from nonlinear best-fit analysis of UV-melting profiles, for the unmethylated  $h26:Y11$  triplex (1). A plausible explanation of this effect is that the methyl group should fill a space in the major groove of  $h26$ , causing a release of hydrating water molecules from the double helix to the bulk, a source of positive entropy change. It has been observed that methylation of cytosine in  $C^5$  also enhances the stability of double-stranded DNA. For instance, the effect of substituting, in the stem of hairpin CGCGCGTTTCGCGCG, the cytosines with 5-methylcytosines, enhances the  $T_m$  from  $74^\circ$  to  $82^\circ\text{C}$ , while the  $\Delta H$  of both hairpins is  $-213\text{ kJ/mol}$  (26). Similarly, in 3 mM NaCl the  $T_m$  values for poly(G-C) and poly(G-5meC) are  $86.5^\circ$  and  $92.2^\circ\text{C}$  respectively, while the  $\Delta H$  per base pair is  $-36$  and  $-37\text{ kJ/mol}$ , respectively (27).

As shown by the thermal behaviour of  $h26:5meY11$  as a function of DNA concentration, the triplex formation is a typical bimolecular process: over a 92-fold DNA concentration range, the reciprocal  $T_{max}$  values depend linearly from  $\ln C_t$ . Since, at a heating rate of  $0.5^\circ\text{C}/\text{min}$ , transition 1 is reversible, the slope and y-intercept provide values for  $\Delta H_t = -27430\text{ kJ/mol}$  and  $\Delta S_t = -78480\text{ J/kmol}$ . A similar analysis, but within a 10-fold DNA concentration range, has been reported by Pilch et al. (28). The calorimetric  $\Delta H_t$  and  $\Delta S_t$  for the triplex to hairpin plus  $5meY11$  transition are  $-23724\text{ kJ/mol}$  and  $-75875\text{ J/kmol}$ ; they are somewhat lower but still within a 15% error in accordance with the van 't Hoff  $\Delta H$  obtained from the  $T_m$  dependence of transition 1 from the DNA concentration. From these values one finds that each pyrimidine residue of  $5meY11$  binding to the major groove of the double-stranded stem helix of  $h26$  is accompanied by:

$\Delta H_t = -21.5 \pm 2.1\text{ kJ/mol}$ ;  $\Delta S_t = -68.9 \pm 6.8\text{ J/kmol}$ ; from DSC  
 $\Delta H_t = -24.9 \pm 2.7\text{ kJ/mol}$ ;  $\Delta S_t = -71.3 \pm 7.2\text{ J/kmol}$ ; from UV

The formation of hairpin  $h26$  is characterized by enthalpy and entropy changes of  $-35\text{ kJ/mol}$  and  $-98\text{ J/kmol}$  per Watson-Crick (W.C.) base pair (data from DSC). Thus, the enthalpic force driving the formation of a Hoogsteen base pair is lower than that found for a W.C. base pair. This is in keeping with the lower hypochromic effect observed for triplex formation (10%) compared to hairpin formation (15%), suggesting a higher degree of base stacking in the latter. As for the entropy change, the Hoogsteen  $\Delta S$  is less negative than the W.C.  $\Delta S$ . This probably arises from a higher release of structured water upon triplex formation, with respect to duplex formation.

From the variation of the  $T_m$  relative to transition 1 ( $h26:5meY11 = h26 + 5meY11$ ) with pH, the proton uptake ( $\Delta nH^+$ ) between hairpin  $h26$  plus  $5meY11$  and the triplex is estimated according to the following relation (29):

$$dT_m/d\log[H^+] = -(\Delta nH^+) 2.303 RT_m^2/\Delta H_t \quad [6]$$

where R is the gas constant. By plotting  $1/T_m$  versus pH, a linear plot is obtained (Figure 7), whose slope,  $-(2.303 R\Delta nH^+)/\Delta H_t$ , allows to estimate the parameter  $\Delta nH^+$ , provided that the enthalpy change of the reaction is known. Using the average between calorimetric enthalpy and van 't Hoff enthalpy ( $\Delta H_t = -255\text{ kJ/mole}$ ), one can estimate from the experimental slope ( $2.3 \times 10^{-4}$ ) that  $\Delta nH^+$  lies around 3. This value is lower than the number of cytosines of  $5meY11$ , since near pH 5 a not negligible fraction of cytosines is protonated, even if  $5meY11$  is not bound to  $h26$  (see Figure 2B).

Two studies on the thermodynamics of triple helix formation by DSC measurements appeared recently in the literature. The first, by Ohms & Ackermann (30), reports the formation of RNA triple helices by  $A_xU_y$  oligonucleotides. The authors found that each U residue binding ( $A.U$ ) $_n$  duplexes is characterized by an average  $\Delta H$  of  $-21.5\text{ kJ/mole}$ , in full accord with the results of this study and the results of previous work from this laboratory (21). In the second study, by Plum et al. (31), it has been found that a 15-mer pyrimidine strand, with a cytosine contents of 33.3%, binds a 21-mer duplex with a  $\Delta H_t = -127\text{ kJ/mole}$  of 15-mer DNA, which means a  $\Delta H_t = -8.4\text{ kJ/mole}$  for each pyrimidine residue. This value is remarkably lower than the  $\Delta H$ s reported in this and our earlier work (21). We feel that this discrepancy is mainly due to the fact that the authors conducted their analysis at a higher pH value (pH 6.5), where the stability of their triplex is much lower.

## ACKNOWLEDGMENT

This work has been carried out with the financial support from MURST (Italy), National Research Council (CNR) and the Netherland Organization for Pure and Advanced Research.

## REFERENCES

- Manzini, G., Xodo, L.E., Gasparotto, D., Quadrioglio, F., van der Marel, G.A. and van Boom, J.H. (1990) *J. Mol. Biol.* **213**, 833–843.
- Le Doan, T., Perrouault, L., Praseuth, D., Hahboub, N., Decout, J-L., Thouong, N.T., Lhomme, J. and Hélène, C. (1987) *Nucl. Acids Res.* **15**, 7749–7760.
- Moser, H.E. and Dervan, P. (1987) *Science* **238**, 645–650.
- Lyamichev, V.L., Mirkin, S.M., Frank-Kamenetskii, M.D. and Cantor, C.R. (1988) *Nucl. Acids Res.* **16**, 2165–2178.
- Praseuth, D., Perrouault, L., Le Doan, T., Chassignol, M., Thoung, N.T. and Hélène, C. (1988) *Proc. Natl. Acad. Sci. USA* **85**, 1349–1353.
- Maher III, L.J., Wold, B. and Dervan, P. (1989) *Science* **245**, 725–730.
- Arnott, S. and Selsing, E. (1979) *J. Mol. Biol.* **88**, 509–521.
- Michelson, A.M., Massoulié, J., Gushulbauer, W. (1967) *Prog. Nucleic Acids Mol. Biol.* **6**, 83–141.
- Morgan, A.R., Wells, R.D. (1968) *J. Mol. Biol.* **37**, 63–80.
- Rajagopal, P. and Feigon, J. (1989) *Nature (London)* **339**, 637–640.
- De los Santos, C., Rosen, M. and Patel, D. (1989) *Biochemistry* **28**, 7282–7289.
- Wells, R.D., Collier, D.A., Hanvey, J.C., Shimizu, M. and Wohlrab, F. (1988) *FASEB J.* **2**, 2939–2949.
- Lyamichev, V.I., Mirkin, S.M. and Frank-Kamenetskii, D.M. (1986) *J. Biomol. Struct. Dynam.* **3**, 667–669.
- Mirkin, S., Lyamichev, V.I., Drushlyak, N.K., Dobrynin, V.N., Filippov, S.A., Frank-Kamenetskii, M.D. (1987) *Nature (London)* **330**, 495–497.
- Hanvey, J.C., Shimizu, M. and Wells, R.D. (1988) *Proc. Natl. Acad. Sci. USA* **85**, 6292–6296.
- Htun, H. and Dahlberg, J.E. (1988) *Science* **241**, 1791–1796.
- Glaser, R.L., Thomas, G.H., Siegfried, E., Elgin, S.C.R. and Lis, J.T. (1990) *J. Mol. Biol.* **211**, 751–761.
- Cooney, M., Czernuszewicz, G., Postel, E.H., Flint, S.J. and Hogan, M.E. (1988) *Science* **241**, 456–459.
- Hélène, C., Thuong, N.T., Saison-Behmoaras, T. and Francoise, J-C. (1989) *Trends in Biotechnology* **7**, 310–315.

20. Lee, J.S., Woodsworth, M.L., Latimer, L.J.P. and Morgan, A.R. (1984) *Nucl. Acids Res.* **12**, 6603–6614.
21. Xodo, L.E., Manzini, G. and Quadrifoglio, F. (1990) *Nucl. Acids Res.* **18**, 3557–3564.
22. Van der Marel, G.A., van Boeckel, C.A.A., Wille, G. and van Boom, J.H. (1981) *Tetrahedron Letters* **22**, 3887–3890.
23. Cantor, C.R. and Schimmel, P.R. (1980) *Biophysical Chemistry, Part II*, W.H. Freeman and Co, San Francisco.
24. Job, P. (1928) *Anal. Chim. Acta* **9**, 113–134.
25. Maher III, L.J., Dervan, P.B. and Wold, B.J. (1990) *Biochemistry* **29**, 8820–8826.
26. Xodo, L.E., Manzini, G., Quadrifoglio, F., van der Marel, G.A. and van Boom, J.H. (1991) *Nucl. Acids Res.*
27. Klump, H.H. and Loffler, R. (1985) *Biol. Chem. Hoppe-Seyler* **366**, 345–353.
28. Pilch, D.S., Brousseau, R. and Shafer, R.H. (1990) *Nucl. Acids Res.* **18**, 5743–5750.
29. Record, M.T., Anderson, C.F. and Lohman T.M. (1978) *Q. Rev. Biophys.* **11**, 103–134.
30. Ohms, J. and Ackermann, T. (1990) *Biochemistry* **29**, 5237–5244.
31. Plum, G.E., Park, Y-W, Singleton, S.F., Dervan, P.B. and Breslauer, K.J. (1990) *Proc. Natl. Acad. Sci USA* **87**, 9436–9440.
32. Xodo, L.E., Manzini, G., van der Marel, G.A., van Boom, J.H., Quadrifoglio, F. (1988) *Biochemistry* **27**, 6327–6331.